Pilot facility for the study of thermal energy storage: Experiments and Theoretical model

A. Castro-Vizcaíno[1,2], K. Babul[3], M.S. Romero-Cano[1,2], J.L. Bosch[1,2], M.J. Ariza[1,2], J. Alonso-Montesinos[1,2], A.M. Puertas[1,2], B. Gil[4], S. Rosiek[4]

[1] Department of Chemistry and Physics, University of Almería, Ctra. Sacramento s/n, Almería, 04120, Spain

[2] CIESOL, Joint Centre of the University of Almería-CIEMAT, Ctra. Sacramento s/n, Almería, 04120, Spain

[3] Department of Energy Conversion Engineering, Wroclaw University of Science and Technology, Wybrzeze Wyspianskiego 27, Wroclaw, 50370, Poland

[4] Department of Thermodynamics and Renewable Energy Sources, Wroclaw University of Science and Technology, Wybreze Wyspianskiego 27, Wroclaw, 50370, Poland

Abstract

Thermal energy storage is a widely used solution to address the mismatch problems between energy availability and demand. However, research in this topic is still necessary to optimise the benefits of energy storage. Here, we present an experimental setup to study the charging and discharging of thermal energy in a storage tank intended for refrigeration. The facility consists of a chiller which cools down the heat transfer fluid (water/glycol mixture), an 80-litres inertia bath to enhance the chiller's cooling capacity, and a storage tank of 60 litres. A three-way valve allows to control the inlet storage tank temperature, and an electric heater is used with the purpose to study the tank discharging process. A theoretical model representing the energy balance equations for each component is also presented to rationalise the experimental results. The model reproduces satisfactorily the operation of the system and shows that even minimal thermal losses must be accounted for, and their relevance in the calculation of the energy balance is shown. Finally, a complex experiment, consisting of three continuous charging-discharging cycles, is analyzed, confirming the validity of the model and its predictive power.

Keywords: Thermal energy storage, pilot facility, thermodynamic modelling

1. Introduction

The demand for energy in the development of our societies is continuously increasing during the last few decades, while this is in stark contrast with the necessity to reduce CO_2 emissions. This combination has been the driving force for research in renewable energies and energy storage. Buildings is one of the sectors where the demand is increasing more rapidly, amounting to 132 exajoules in 2021, around 30% of the global energy consumption, according to the REN21 Global Status Report (Ren21, 2023), and around 75% of this demand is used for space heating and cooling. However, only 14% of the heating demand was covered with renewable energy in 2021, mainly due to the intermittency of the energy source and the mismatch between energy production and demand, in comparison to the easiness and fastness of fossil fuels-based technologies. Thermal energy storage appears therefore as a suitable tool to cover this mismatch and boost the use of renewable sources in heating and cooling applications (Cabeza, 2022; Lizana, 2018).

Several strategies have been developed, but the most widely extended ones are storing the thermal energy in the form of temperature variations of a substance (sensible heat) or inducing a phase change in a so-called phase change material, PCM, (Alva, 2018). Although the use of thermal energy storing is common in many different applications, there are still many aspects that need further research, such as the internal structure of the tanks, the control strategies, or the development of new materials. For this purpose, many researchers have designed pilot plants that allow the study of small storage systems (Zhang, 2016). The analysis of the results

10.18086/eurosun.2024.06.03 Available at http://proceedings.ises.org

from these experiments is then scaled up into real applications, but this requires a deep understanding of the pilot facility. For instance, Koukou et al. (Koukou, 2020) built a prototype storage system based on PCMs, and with two different energy sources, solar and geothermal energy. Two different PCMs were tested, and the most stable output is proposed as optimal for their application. Weiss et al. (Weiss, 2021) studied numerically the stratification inside a tank to conclude that the idealised flow distribution misestimated the thickness of the thermocline and optimised the inlet location for their application. In refrigeration applications, Selvnes et al. (Selvnes, 2021) designed and tested a novel plates-in-tank storage unit, integrated in a pilot facility modelling industrial refrigeration systems based on CO_2. Oró et al. (Oró, 2012) used a pilot plant to study the optimal design of an energy storing system in the high temperature inlet to an absorption, adsorption, or desiccant chiller. Even more, the combination of modelling and experiments improves the understanding of an actual facility, in particular for the analysis of heat losses in a storage tank, as performed by Mawire (Mawire, 2013). These few examples show that this field is still under development, mainly due to the many different processes involved in it. Further cases can be found in the recent review papers (Elalfy, 2024; Li, 2019; Mitali, 2022).

In this work, we present a pilot facility for the study of a storage tank of 60 litres, aimed for the analysis of PCMs as storage medium for refrigeration (the whole system operates at sub-zero temperatures). It is composed of a chiller unit and a buffer, or inertia, bath of 80 litres, a heater, and the storage tank. In the present work and with the main goal to simplify the experiments and theoretical description, the storage tank does not contain PCMs, and only the heat transfer fluid (HTF) is used as a storage medium. The system allows setting the mass flow rate and storage inlet temperature, as well the heater to simulate an external load to activate the tank discharging process. Moreover, a theoretical model is also presented, based on the energy balance of the main components of the facility, where most of the parameters are taken from the real experiment. The comparison of the model with the experiments shows that even minimal thermal losses must be considered in the storage design process, therefore its importance when we compare to the total energy stored in the tank were also presented.

This work is part of the European Life Programme project COOLSPACES 4 LIFE, aimed to test the viability of thermal PCM-based energy storage for a newly developed solar powered air conditioning system.

2. Materials and methods

2.1. Technical data

Figure 2.1 illustrates the pilot unit of the cooling system, which consists of an inertia tank, an electric heater, two circulation pumps, two- and three-way valves, and the corresponding piping. Panels (b) and (c) show the storage tank from side and top views, respectively. Additionally, Figure 2.2 provides a schematic representation of the system's components and the complete hydraulic layout. A glycol/water mixture at a 70/30 ratio was employed as the heat transfer fluid (HTF). The cooling unit, with a rated cooling capacity of 1.7 kW, operates based on a conventional vapor-compression refrigeration cycle. This is composed of a compressor, a condenser, an expansion valve, and an evaporator, along with the R449A refrigerant. Its temperature operating range varies from -40 ºC to +100 ºC and can withstand pressures up to 28 bars. The buffer tank has a storage capacity of 80 litres. An electric heater with a maximum power of 2 kW is used for the discharge process of the storage tank. The circulation pumps allow variable flow rates, varying the electricity power from 18 W to 191 W. The inertia tank and all conduits are thermally insulated with elastomeric foam to minimize heat exchange with the environment.

The right section of the experimental setup (c.f. Figs. 2.1 b and c) presents the horizontal thermal storage tank that was designed for sensible or latent heat storage. This work focuses only on sensible heat storage operation conditions, while latent heat storage experimental results will be presented elsewhere. The presented storage tank was designed within the COOLSPACES 4 LIFE project and manufactured by one of consortium partners, Hedera Helix. Constructed from stainless steel, the tank's dimensions are 750 mm x 400 mm x 200 mm, with a total volumetric capacity of 60 litres. It is equipped with small observation windows to monitor the fluid dynamics. For precise temperature control, six holes in one side of the tank facilitate the insertion of six probe branches with racor connections to prevent HTF leaks. This design allows the accommodation of up to 32 temperature probes. To mitigate fluid stratification, the tank incorporates eight fluid inlets, four at the upper and lower levels, with an equivalent configuration at the tank outlet. An access gate is installed at the top of the tank, enabling the manipulation of internal probes and encapsulated phase change materials (EPCMs) for future experimental applications. Thermal insulation is provided by an external layer of polyurethane insulating foam surrounding the whole tank, except the observation windows and gate.

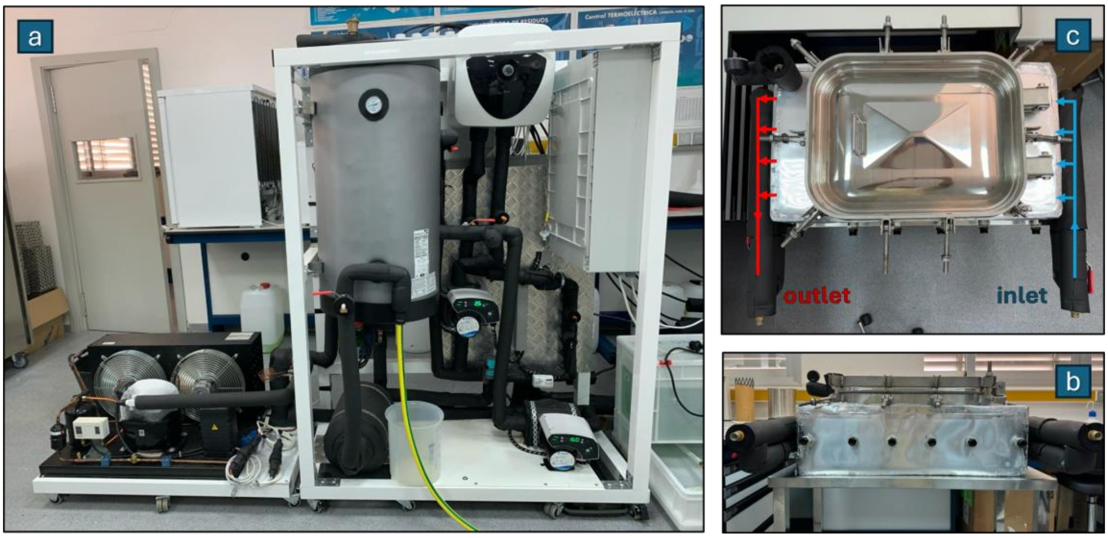

Fig. 2.1: Photograph of the experimental cooling setup with the buffer tank and the heater on the left and a top view of the horizontal storage tank on the right (c) along with a front view (b).

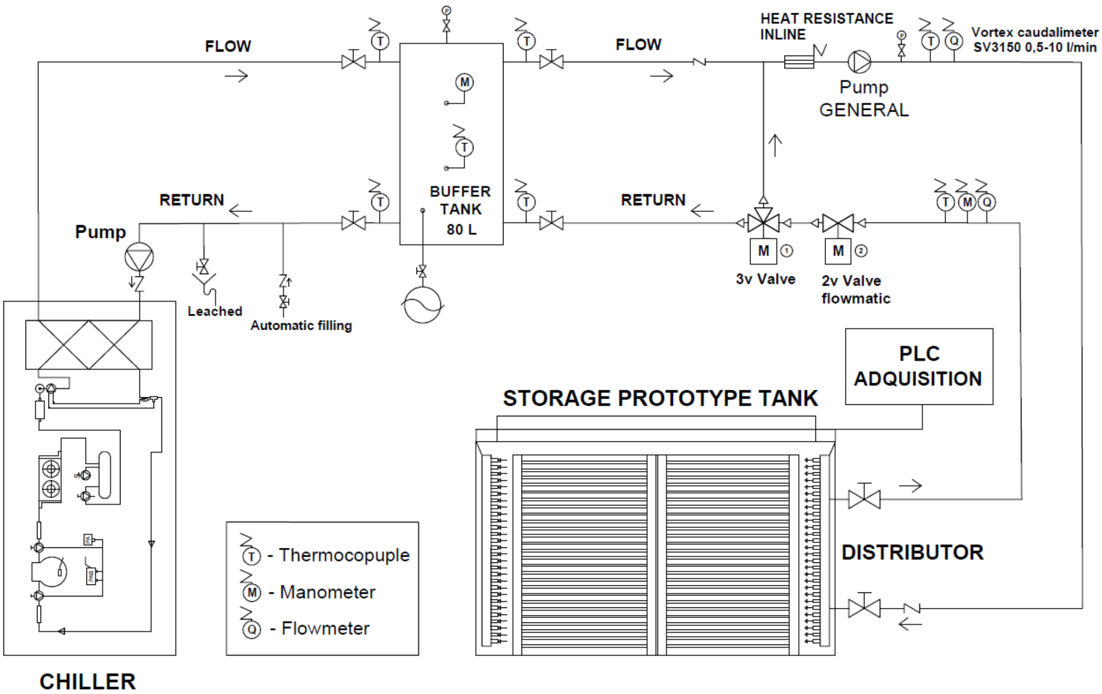

Fig. 2.2: Scheme of the components and hydraulic layout of the system.

For the inlets, outlets, and the interior of the inertia tank, NTC Type JIC probes are utilized. These probes operate within a temperature range of -50 °C to 105 °C and have a tolerance of ±0.1°C. In the rest of the circuit, TA2105 probes are employed, which feature a Class A PT1000 sensor. These probes offer a measurement range of -50 °C to 150 °C with a sensitivity of ±0.1°C.

Inside the pilot tank, T-type thermocouples from Omega are used. These thermocouples have epoxy-coated tips, making them suitable for humid and oxidizing environments. They operate within a temperature range of

-200 °C to 350 °C. When integrated into our control system, the thermocouples exhibit an error margin of ±0.1°C, despite their inherently higher precision and sensitivity.

The flowmeter employed is the SV3150 model from ifm electronic gmbh, which is compatible with glycol-based solutions. It has an operating temperature range of -40 °C to 100 °C and a maximum pressure capacity of 12 bar. This flowmeter utilizes the vortex measurement principle and supports flow rates between 0.5 and 10 L/min, with an error margin of 0.2%.

2.2. Operation mode

The experimental set-up can operate in two different modes: charging mode –cold HTF entering in the storage tank which is initially hot, extracting heat and cooling it down– as well discharging mode –hot HTF entering in the storage tank, initially cold, and where the cold fluid stored in the tank is circulated through an electrical resistance which simulates a constant energy demand. This dual-mode operation allows the prototype to serve as a scalable model for real-world applications in thermal energy storage systems, particularly for air-conditioning systems in buildings. A detailed description of both operational modes is provided below.

Charging Mode:

This mode starts with the pre-cooling of the heat transfer fluid (HTF) that circulates through the entire system. This cooling is achieved by a heat exchanger in the chiller unit, specifically the evaporator of the cycle. As the HTF cools, (negative) energy is accumulated in the buffer tank until it reaches the set point (T_{buffer}), while keeping the storage tank at a controlled higher temperature. Once the buffer tank is charged, the actual charging of the thermal storage tank begins, using the energy stored in the buffer tank while the chiller tries to keep its temperature to the set point. The temperature of the inlet to the storage tank (T_{inlet}) is fixed (above the temperature of the inertia bath) using the three-way valve, mixing the outlet of the storage and buffer tanks. This operational mode is designed to minimise the charging time. A hysteresis mechanism is used in the buffer tank to allow variations of the temperature around the set point without the chiller working.

Discharging Mode:

When the thermal storage tank is charged, it can be discharged using the heater. This operation mode involves closing the 3-way valve to circulate the HTF against a variable load resistance (fixed load during each test), thereby dissipating all the stored energy during the charging process and simulating a real discharging operation.

For both operation modes, the parameters that the user can modify include: buffer tank temperature, inlet temperature to the storage tank, system flow rate, power of the general pump, opening or closing of the three-way valve and the percentage of load offered by the resistance. The system flow rate is controlled by the power of the general pump and the two-way valve located at the storage tank outlet, which operates automatically based on the integrated control system. To control the inlet temperature to the storage tank, the three-way valve operates to regulate the mixture between the storage tank outlet and the buffer tank outlet, thereby adjusting the temperature to the selected set value. When the system operates in discharging mode, the valve must be closed to 0% to isolate the buffer tank and prevent the mixture of the HTF from the buffer and storage tanks.

3. Model description

In order to model the experimental setup described previously, it is schematized as shown in Fig. 3.1. For all components, the energy balance equation is used:

$$\frac{dE_{vc}}{dt} = \dot{Q} - \dot{W} + \sum_{e} \dot{m}_e h_e - \sum_{s} \dot{m}_s h_s \tag{1}$$

where E_{vc} stands for the energy in the control volume, $\dot{Q}$ corresponds the heat power exchanged through the boundaries, $\dot{W}$ is the power developed within the control volume, and equal to zero in all our components, and $\dot{m}$ is the mass flow rate. The subindices *e* and *s* refer to “entering” and “leaving” the control volume. The approximation of subcooled liquids is used due to the small changes of temperature, allowing us to calculate the change in enthalpy as $\Delta h = c_p \cdot \Delta T$.

In the cooling unit, only the heat exchanger is considered, with a cooling capacity $\dot{Q}_{cooler}$. Ideal mixing is assumed in both the *inertia bath* and the *storage tank*, and heat gains from the environment are included, proportional to the temperature difference with the ambient. The three-way valve is also included, with a control similar to the experimental setup, to achieve the target temperature entering the *tank*, T_{3a}. The heater is active only in the discharging mode and is characterised by the thermal power $\dot{Q}_{heater}$.

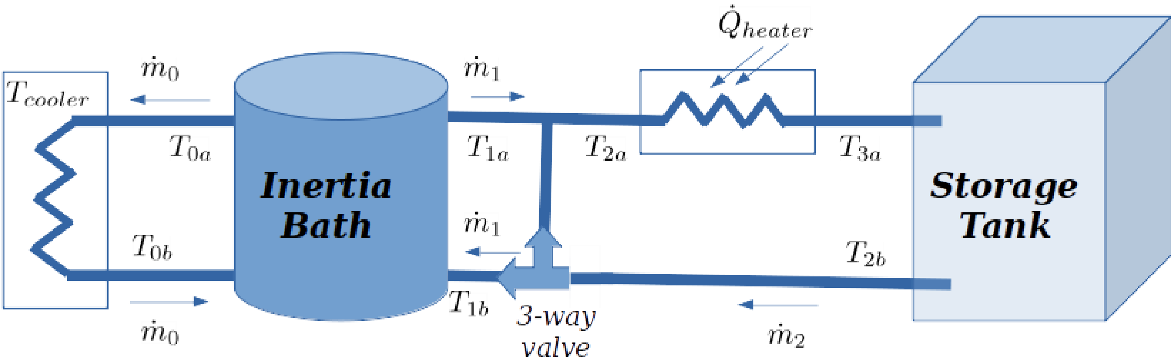

Fig. 3.1: Schematic representation of the experimental setup, with the variables for the model.

The governing equations, derived from Eqn. (1) for every component of the setup, are therefore as follows (note that $\dot{W}$ is zero in all cases):

- Cooler. This is simulated as a heat exchanger between the HTF and the refrigerant. The heat absorbed by the refrigerant, at temperature T_{cooler}, is given by $\dot{Q}_{cooler} = k(T_{cooler} - T_{0a})$, where k is a heat transfer coefficient to be determined. Assuming that the cooler is in the stationary state, the temperature of the HTF leaving the cooler is:

$$T_{0b} = T_{0a} + \frac{k}{\dot{m}_0 \cdot c_{HTF}}(T_{cooler} - T_{0a}) \tag{2}$$

  with c_{HTF} the specific heat capacity of the HTF. Note that because $T_{cooler} < T_{0a}$, the output temperature T_{0b} is lower than the inlet, T_{0a}.

- Bath. The inflows with temperatures T_{0b} and T_{1b} mix ideally, and the temperature of the outlets are equal, and identical to the bath temperature: $T_{0a} = T_{1a} = T_{bath}$. Using that the energy variations within the tank are given by $dE_{vc} = m_{bath}\, c_{HTF}\, dT_{bath}$, the evolution of the bath temperature is given by:

$$\frac{dT_{bath}}{dt} = \frac{\dot{m}_0}{m_{bath}}(T_{0b} - T_{bath}) + \frac{\dot{m}_1}{m_{bath}}(T_{1b} - T_{bath}) + \frac{\dot{Q}_{env}}{m_{bath} \cdot c_{HTF}} \tag{3}$$

  where m_{bath} is the HTF mass inside this tank. The heat gain from the environment is also included, calculated as:

$$\dot{Q}_{env} = k_{env}(T_{bath} - T_{env}) \tag{4}$$

  with k_{env} a constant that controls the heat exchange.

- 3-way valve. This is used to fix the temperature T_{3a} in the charging mode, without any energy exchange. The opening of the valve is calculated as:

$$x_v = \frac{T^*_{tank} - T_{tank}}{T_{bath} - T_{tank}} \tag{5}$$

where T^*_{tank} is the set point of the tank; when x_v, calculated with this equation is larger than one, it is set to one. The mass flow rate entering the inertia bath from the storage tank is then set according to $\dot{m}_1 = x_v \cdot \dot{m}_2$.

In the discharging mode, in contrast, x_v is fixed $x_v = 0$, and the heater is connected.

- Heater. To model the electric resistance, only the heat flux to the HTF is considered, and it is assumed to work in the stationary state. Thus:

$$T_{3a} = T_{2a} + \frac{\dot{Q}_{heater}}{\dot{m}_2 . c_{HTF}} \tag{6}$$

where $\dot{Q}_{heater}$ is the heat transferred to the HTF per unit time, which is assumed to be equal to the power of the electric resistance.

- Storage tank. This reservoir is intended to store the energy, either using sensible heat (with HTF or another material), or latent heat with PCM. In this case, energy is stored in the HTF. Using again that $dE_{vc} = m_{tank}\, c_{HTF}\, dT_{tank}$, the energy balance in the tank results in:

$$\frac{dT_{tank}}{dt} = \frac{\dot{m}_2}{m_{tank}}(T_{3a} - T_{tank}) + \frac{\dot{Q}_{env}}{m_{tank} . c_{HTF}} \tag{7}$$

where the heat gain from the environment is calculated as in Eqn. (4), with the tank temperature instead of the buffer tank temperature. The parameter k_{env} is similar in both cases, for simplicity.

The system of equations formed by equations (2), (3), (4), (6), and (7) with the relation between the mass flow rates with x_v, is solved numerically, obtaining the evolution of all temperatures as a function of time, and allowing a direct comparison with the experiments. This requires the specification of T_{cooler}, k and k_{env}, which cannot be accessed experimentally, whereas the flow rates, mass of HTF in the buffer and storage tanks, and power of the heater are taken from the experimental setup, as well as the initial conditions. The time step is set to δt = 1s, which was checked to be small enough not to influence the results.

4. Results

Fig. 4.1 depicts the results of a single experiment and its comparison with the theoretical model presented in the previous section. The initial part of the graph (for times below 770 min) shows the cooling of the inertia bath, until it reaches a low enough temperature to start the charging experiment. At t = 770 minutes, the HTF is directed to the storage tank, while the primary loop keeps cooling the bath. At t = 1270 minutes, the tank has been fully charged as noted by the outlet temperature, which is constant, and the discharging process starts with the heater, with a power set to 2000 W. The 3-way valve is closed, and the inlet temperature raises notably. During the charging process, the constant difference between the inlet and outlet temperatures (green and blue points) a long times, indicates that there is a constant input of energy in the tank; these are the thermal gains from the environment.

The predictions of the model are shown by the lines in the figure, with T_{cooler} = -20.5 ºC, $k = 110\ W\ K^{-1}$ and $k_{env} = 14\ W\ K^{-1}$ (the rest of parameters are taken from the experiment, in particular $\dot{m} = 0.069\ Kg/s$). Note that the model reproduces correctly the evolution of the temperatures in the buffer tank and the storage tank inlet and outlet temperatures. Notably, the increase of the buffer tank temperature when the charging starts (bump in the red curve at times around 800 min.) is reproduced, as well as the difference between the inlet and outlet temperatures. On the other hand, the light green points in the figure represent the average temperature inside the tank, which lies between the inlet an outlet temperatures during the charging.

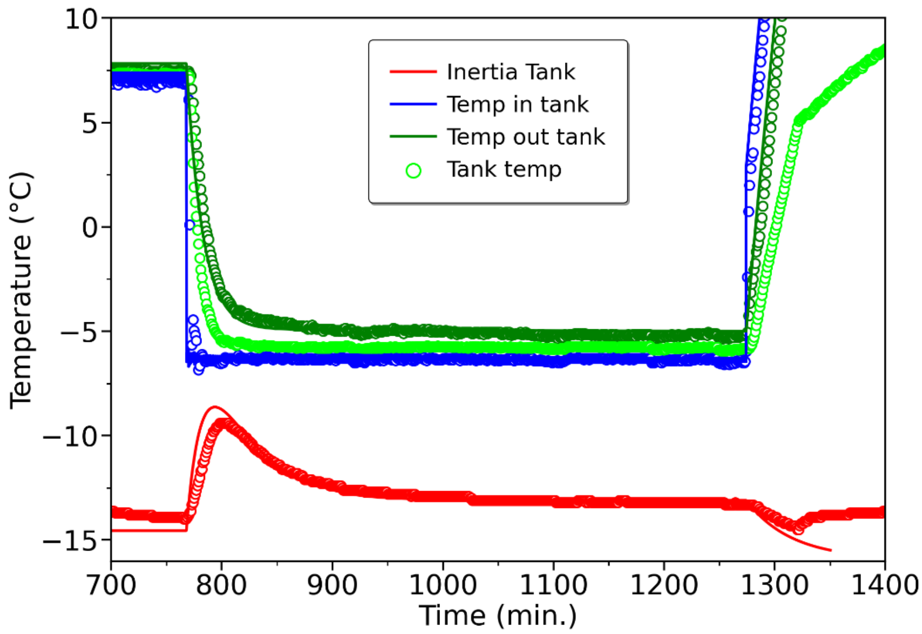

Fig. 4.1: Experimental evolution of the temperature in the inertia bath (red line), inlet and outlet to the storage tank (blue and green lines, respectively).

The energy stored in the tank can be calculated from the energy balance from the temperature of the inlet and outlet flows. The total energy is given by:

$$E_{vc} = \int_{t_0}^{t_1} dt\, \dot{m} c_{HTF} \cdot (T_{3a} - T_{2b}) \tag{8}$$

Note that since $T_{3a} < T_{2b}$ during the charging, this energy is negative. However, only a fraction of this energy is stored in the tank, whereas the rest is dissipated to the environment (gains from the environment cancel it).

Fig. 4.2 shows the evolution of the energy balance (in absolute value) for the same case as presented above, comparing the experiments and simulations. The agreement between the both energy balances is excellent, as expected by the good agreement of the temperatures shown previously. The horizontal line in the graph shows the energy that can be stored according to the change of HTF temperature:

$$Q = m_{tank} \cdot c_{HTF} \cdot \Delta T \tag{9}$$

and the green line shows the energy that is truly stored in the tank, according to the model (substracting the exchange with the environment). This approaches the value given by Eqn. (9) at long times, showing that the tank is fully charged in approximately 100 minutes, although in our experiment the charging extends for around 500 minutes. Therefore, a large fraction of the (negative) energy introduced in the tank is compensated by the energy gains from the environment.

After the tank has been charged, it is discharged with the heater, as mentioned above, and the energy in the tank starts decreasing. After 40 minutes, the outlet temperature reaches the initial temperature of the storage tank, 7 ºC. The difference between the energy when the discharging starts, and this point, is the energy that is recovered in this experiment, which should agree with the stored energy (horizontal line in the figure).

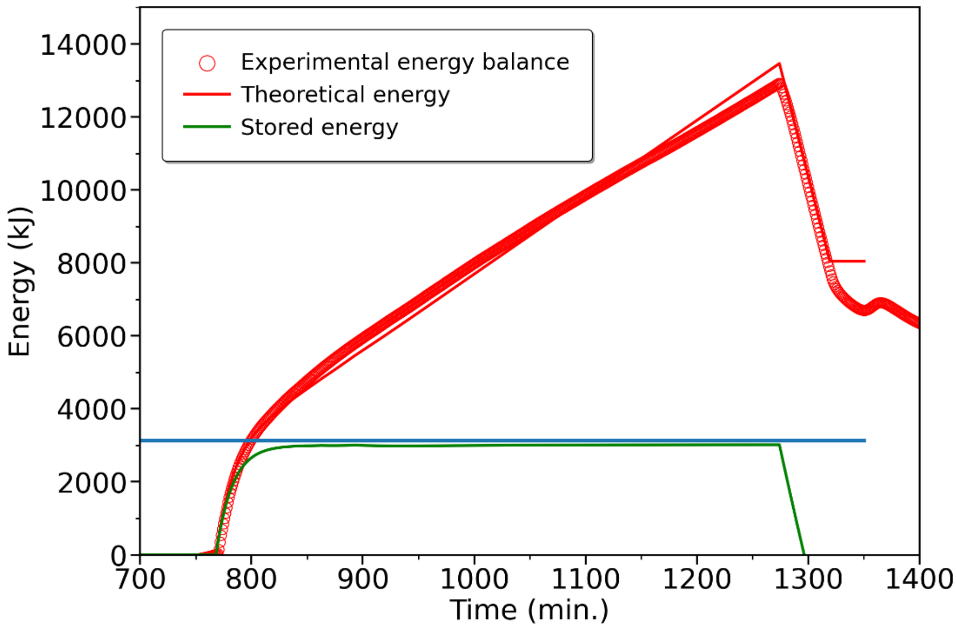

Fig. 4.2: Energy transferred into the storage tank, experimentally (circles) and from the model (line). The horizontal line represents the energy stored in the HTF according to eq. (9), and the green line represents the energy stored in the tank, according to the model.

Fig. 4.3 shows the energy driven to the storage tank calculated from the experiment and model, and the energy recovered experimentally during the discharging phase. Different experiments, with different inlet temperatures are shown, and the calculation of the sensible energy in the HTF, Eqn. (9), is also included. The energy recovered is much smaller than the energy introduced, but follows the calculation of the sensible energy, showing clearly that most of the energy introduced in the tank is dissipated. Also, the graph shows that the energy calculated with the model agrees quite well with the experimental calculations.

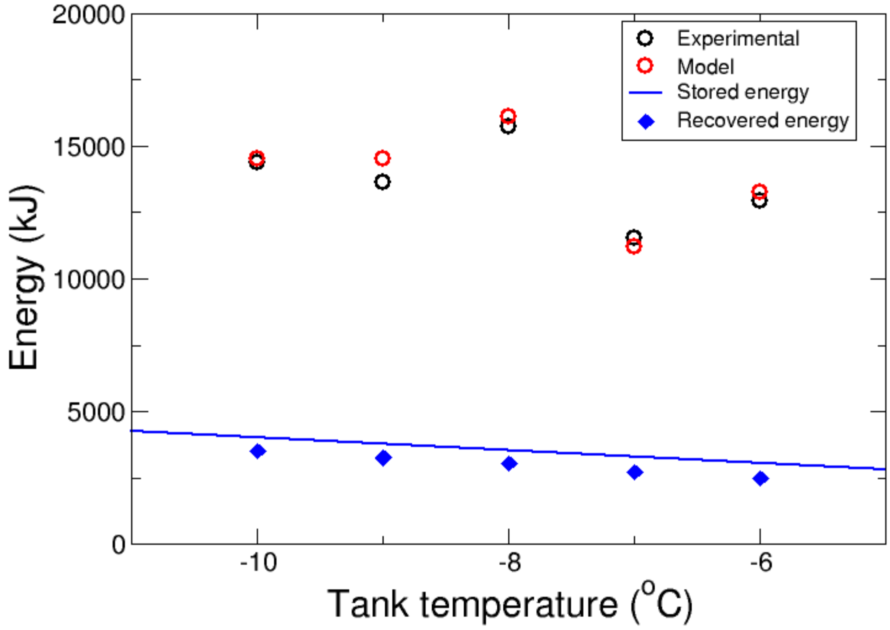

Fig. 4.3: Energy transferred into the storage tank, experimentally (black circles) and from the model (red circles), as a function of the set point tank temperature. The line represents the store capacity according to eq. (9), and the blue diamonds show the energy that is recovered.

4.1. Cyclic operation

An energy storage system is expected to work periodically, in constant cycles of charging and discharging. Therefore, the pilot tank studied here was subjected to continuous cyclic operation, and the performance of the model was studied. Fig. 4.4 shows the evolution of the bath and tank temperatures experimentally (points) and in the theory (lines). The charging and discharging times in the model have been set from the experiments, as well as the HTF flow rate, set point temperatures and resistance power. The overall agreement is very good, with slight differences in the bath temperature, which affect the tank inlet, and the maximum temperature during the discharging. This graph exemplifies that the parameters fitted previously are valid in other cases, and can be used to model the behaviour of the system.

In Fig. 4.5 the (negative) energy balance in the tank during the cycling is shown, calculated from the experimental inlet and outlet temperatures, and from the model predictions. Both results agree over the whole time range. Additionally, the blue line shows the energy stored in the tank, which grows to the maximum level (calculated according to the tank temperature), and decreases again when it discharges; the green line shows the energy gains from the environment, which grow continuously with time. This confirms that the tank charges and discharges completely in every cycle. Note that the first charging has been extended over 4 hours, because the outlet of the tank was decreasing. However, the energy balance proves that the change in energy is negligible after the first hour. In the subsequent cycles, the charging takes a bit longer, since the inertia bath is not as cold as in the first cycle. In any case, the model can reproduce the whole behaviour of the temperatures and the energy.

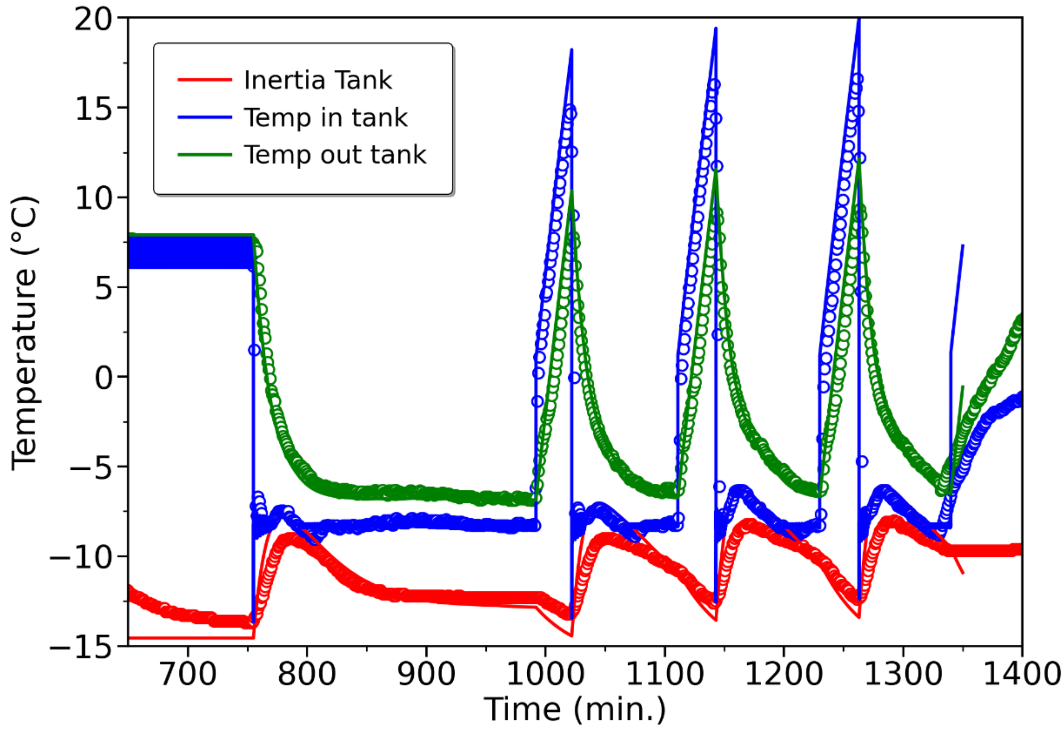

Fig. 4.4: Evolution of the temperature in the inertia bath (red line and points), inlet and outlet to the storage tank (blue and green, respectively) in three continuous cycles.

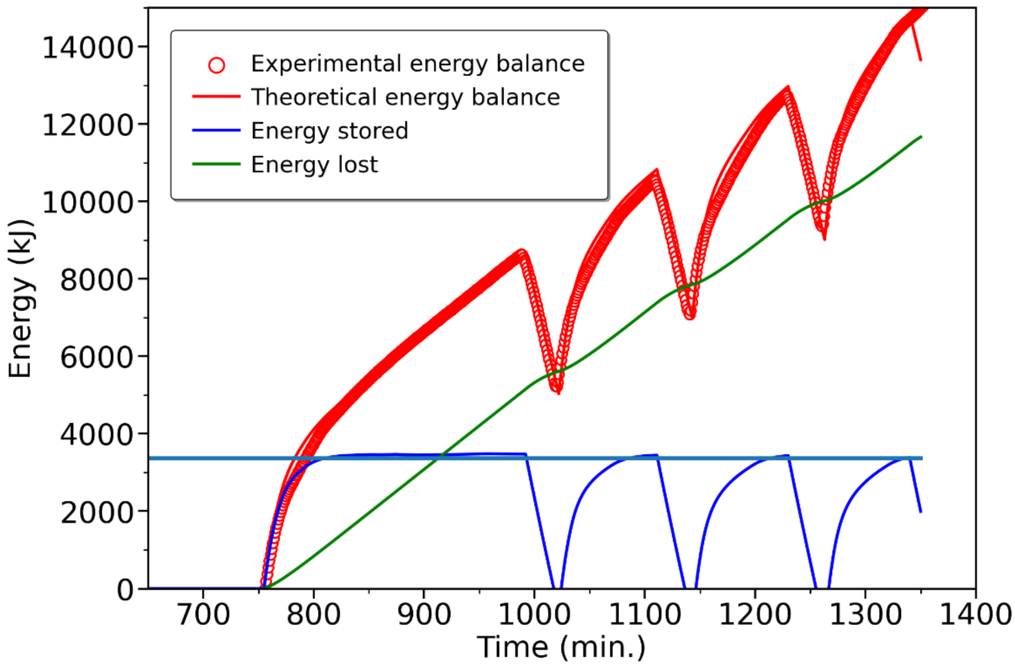

Fig. 4.5: Evolution of the energy in the storage tank: energy balance (red line and points), stored energy (blue line) and energy gains from the environment (green line).

5. Discussion and conclusions

Although the model presented here is very simple, and contains only a limited number of parameters, it provides an acceptable description of the presented pilot facility through the evolution of the temperatures in key locations, and the subsequent analysis of storage tank energy balance. Even more, it has led us to verify and quantify the heat gains from the environment that are necessary for a full interpretation of the experimental results. The prototype is now well understood, with all relevant parameters characterised properly, thus the model can be used to predict its behaviour in different circumstances.

In summary, we have presented a prototype cooling facility connected to a tank intended for thermal energy storage for refrigeration. A model describing the thermal balance of each its component has been used to rationalise the results, with a small number of adjustable parameters. The model has shown that thermal losses, are relevant to interpret correctly the experimental results, allowing to calculate with good agreement between experiments and the model the amount of energy stored in the tank, and dissipated to the environment. A typical cyclic operation of the storage system has also been studied, with excellent agreement between the experiment and the model.

An attractive future work will consist of introducing encapsulated PCM in this pilot storage tank to perform charging and discharging cycles to gain knowledge for full scale tank operation, that will be installed in two institutional buildings in different locations: Almeria (Spain) and Wroclaw (Poland).

6. Acknowledgments

The COOLSPACES 4 LIFE project (LIFE20 CCM/PL/001607) is financed by the European Commission under the LIFE Programme and co-financed by the National Fund for Environmental Protection and Water Management in Poland (Project 2244/2021/WN01/OA-PO-LF/D).

Sabina Rosiek is most grateful for the financial support from the Polish National Agency for Academic Exchange, Polish Returns 2018 (https://nawa.gov.pl/en/), with the project identification number: 07PP/0001/19.

7. References

Alva, G., Lin, Y., Fang G., 2018. An overview of thermal energy storage systems. Energy, 144, 341-378.

Cabeza, M.L. (ed.), 2022. Encyclopedia of Energy Storage (four volumes). Elsevier. (See in particular the first volume for Thermal Energy Storage).

Elalfy, D. A., Gouda, E., Kotb, M. F., Bureš, V., & Sedhom, B. E., 2024. Comprehensive review of energy storage systems technologies, objectives, challenges, and future trends. Energy Strategy Reviews, 54, 101482.

Koukou, M.K., Dogkas, G., Vrachopoulos, M.Gr., Konstantaras, J., Pagkalos, Ch., Stathopoulos, V.N., Pandis, P.K., Lymperis, K., Coelho, L., Rebola, A., 2020. Experimental assessment of a full scale prototype thermal energy storage tank using paraffin for space heating application. International Journal of Thermofluids, 1-2, 100003.

Li, S. F., Liu, Z. H., & Wang, X. J., 2019. A comprehensive review on positive cold energy storage technologies and applications in air conditioning with phase change materials. Applied Energy, 255, 113667.

Lizana, J., Chacartegui, R., Barrios Padura, A., Ortiz, C., 2018. Advanced low-carbon energy measures based on thermal energy storage in buildings: A review.Renewable and Sustainable Energy Reviews, 82, 3705-3749.

Mawire, A., 2013. Experimental and simulated thermal stratification evaluation of an oil storage tank subjected to heat losses during charging. Applied energy, 108, 459-465.

Mitali, J., Dhinakaran, S., & Mohamad, A. A., 2022. Energy storage systems: A review. Energy Storage and Saving, 1(3), 166-216.

Oró, E., Gila, A., Miróa, L., Peiróa, G., Álvarezb, S., Cabeza, L.F., 2012. Thermal energy storage implementation using phase change materials for solar cooling and refrigeration applications. Energy Procedia 30 947–956.

REN21,2023. Renewables 2023 Global Status Report collection, Renewables in Energy Demand. ISBN 978-3-948393-07-6.

Selvnes, H., Allouche, Y., Hafnes, A., 2021. Experimental characterisation of a cold thermal energy storage unit with a pillow-plate heat exchanger design. Applied Thermal Engineering, 199, 117507.

Weiss, J., Ortega-Fernández, I., Müller, R., Bielsa, D., Fluri, Th., 2021. Improved thermocline initialization through optimized inlet design for single-tank thermal energy storage systems. Journal of Energy Storage 42, 103088.

Zhang, H., Baeyens, J., Cáceres, G., Degrève, J., Lv, Y., 2016. Thermal energy storage: Recent developments and practical aspects. Progress in Energy and Combustion Science 53, 1.